Philosophical Magazine B, 1992, Vol. 65, No. 4, 861–866

Percolation approach to proton conductivity in hydrated protein powders

M. Settles†, W. Doster†, F. Kremer‡, F. Post†
and W. Schirmacher†

† Physik-Department E13, Technische Universität München,
W-8046 Garching, Germany
‡ Max-Planck-Institut für Polymerforschung, W-6500 Mainz, Germany

[*Received 21 October 1991 and accepted 25 November 1991*]

Abstract

The dielectric response of hydrated myoglobin powder has been measured in the range 10^6–10^9 Hz. The data reveal at least two distinct processes which are explained by reorientation of water dipoles and conduction of protons along connected patches of water molecules. It is shown that proton hopping may be approximated by a simple percolation model, which predicts an algebraic low-frequency divergence $\varepsilon''(\omega) \propto \omega^{-0\cdot5}$ at the threshold.

§ 1. Introduction

Hydrated protein powders exhibit three regions of dielectric dispersion covering 1 to 10^{10} Hz. The low- and intermediate-frequency processes (1–10^7 Hz) were attributed to bulk conductivity of protons and localized displacements of protons along the surface of individual protein molecules (Careri, Geraci, Giansanti and Rupley 1985, Hawkes and Pethig 1988). The high-frequency loss results from reorientation of sorbed water molecules (Shinyashiki *et al.* 1990). The protonic conductivity measured as a function of the degree of hydration reveals a critical behaviour, which was described in the framework of a percolation model (Careri, Giansanti and Rupley 1986). In this picture the conductivity reflects motion along threads of hydrogen-bonded water molecules. In fact a cross-over from two-dimensional (2D) to three-dimensional (3D) percolation was identified according to the corresponding critical exponents (Careri, Giansanti and Rupley 1988). Long-range 2D displacements become possible above a threshold of $0\cdot15\,\mathrm{g\,g^{-1}}$ indicating a percolating network of water molecules on the protein surface. At full monolayer coverage ($0\cdot35\,\mathrm{g\,g^{-1}}$), the hydration shells of adjacent molecules overlap, which gives rise to bulk conductivity. The experiments and arguments presented above concern essentially the d.c. conductivity. However, a particle performing a random walk on a percolation cluster will encounter dead ends on all length scales. As a consequence the mean square displacement increases sublinearly in time, which gives rise to a frequency-dependent conductivity $\sigma(\omega)$. Scaling arguments suggest $\sigma(\omega) \propto \omega^a$, $a \approx 0\cdot34$ ($D=2$), $0\cdot6$ ($D=3$) independent of the lattice structure (Bunde and Maass 1991). To obtain information on $\sigma(\omega)$, we performed dielectric experiments on hydrated myoglobin close to threshold for 3D percolation at $h = 0\cdot32$–$0\cdot36\,\mathrm{g\,g^{-1}}$. To extend the effective frequency range of the spectrometer (10^6–10^9 Hz), the temperature was varied between 200 and 320 K. This allows in particular to take into account the fast reorientation of water dipoles which also contributes to the spectrum. Our percolation model consists of a 3D network of coordination Z specified by a random distribution of strongly and weakly conducting sites. The frequency-dependent conductivity is calculated using an effective-medium approximation (Movaghar and Schirmacher 1981).

§2. THEORY

Starting with a master equation

$$\frac{\mathrm{d}n_i}{\mathrm{d}t}=-\sum_j W_{ij}n_i+\sum_j W_{ji}n_j \tag{1}$$

for the site occupancy n_i and transition rates W_{ij}, one replaces the real system by an effective system specified by identical but frequency-dependent transition rates $m(p)$, where $p=\mathrm{i}\omega$ denotes a complex frequency. The effective rates depend on W_{ij} through the following self-consistency equation (Doster, Schirmacher and Settles 1990, Doster and Schirmacher 1991):

$$m(p)=Za_p\left\langle\frac{1}{1/[m(p)+p]+1/W_{ij}}\right\rangle. \tag{2}$$

a_p is a density renormalisation constant ($a_p=0{\cdot}368$ for $D=3$), Z the coordination number, and $\langle\ldots\rangle$ denotes the average over a distribution of rates $p(W)$. We now assume a bimodal distribution of rates given by

$$p(W)=x\delta(W-W_0)+(1-x)\delta(W-W_1), \tag{3}$$

with $W_1 \ll W_0$, where x denotes the concentration of connected sites. A finite W_1 accounts for leakage current between disconnected sites. From eqns. (2) and (3) we obtain

$$m(p)=\frac{1}{x_c}\left(x\frac{W_0}{1+W_0/[p+m(p)]}+(1-x)\frac{W_1}{1+W_1/[p+m(p)]}\right). \tag{4}$$

The critical concentration x_c is given by $1/Za_p$. The conductivity $\sigma(p)$ is proportional to the transition rate $m(p)$ which contributes to the dielectric constant according to (Böttcher and Bordewijk 1978)

$$\begin{aligned}\varepsilon'(\omega)&=\varepsilon_1'(\omega)-\frac{\sigma''(\omega)}{\omega\varepsilon_0},\\ \varepsilon''(\omega)&=\varepsilon_1''(\omega)+\frac{\sigma'(\omega)}{\omega\varepsilon_0}.\end{aligned} \tag{5}$$

$\varepsilon_1(\omega)$ refers to non-conductive processes such as water dipole reorientation. Figure 1 shows the resulting $\varepsilon''(\omega)$ ($\varepsilon_1''=0$) above and below the percolation threshold defined by the separation parameter $\delta=(x-x_c)/x_c$. For $\delta>0$, $\sigma(\omega)$ is independent of frequency for $\omega>W_0$ and $\omega<\delta^2W_0$, resulting in $\varepsilon''\propto 1/\omega$. In between there is anomalous dispersion $\varepsilon''\propto\omega^{-0{\cdot}5}$. For $\delta<0$ a maximum appears at $\omega=\delta^2W_0$ because of a vanishing d.c. conductivity. For finite W_1 there is a second low-frequency dispersion. Curve shapes such as those displayed in fig. 1 are often encountered in dielectric measurements on water-containing organic samples (Careri and Giansanti 1984, Hawkes and Pethig 1988). The peak in $\varepsilon''(\omega)$ is usually interpreted as a Maxwell–Wagner dispersion due to localized conduction processes within the sample. Figure 1 also compares $\varepsilon''(\omega)$ of the model with a Cole–Davidson distribution of width $\beta=0{\cdot}5$ which was cut off at $\tau=1/W_0$.

Fig. 1

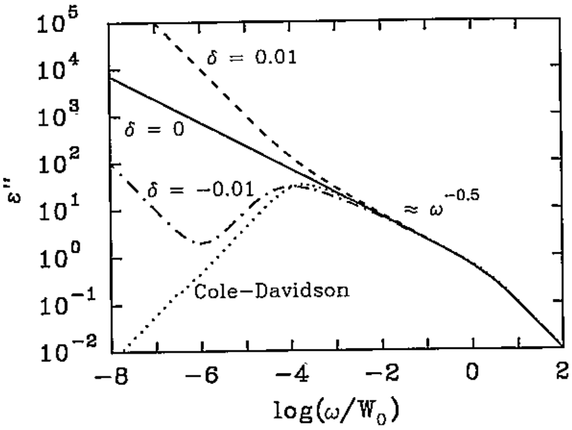

Dieletric loss factor $\varepsilon''(\omega) \propto \sigma'(\omega)/\omega$ according to eqn (4) and $W_1 = 10^{-6} W_0$ for different separation parameters δ. (.....) modified Cole–Davidson distribution, $\beta = 0{\cdot}5$.

To analyse the experiments we further assume a Cole–Davidson distribution for $\varepsilon_1(\omega)$ describing fast reorientation of water dipoles. The complex dielectric constant $\varepsilon(\omega)$ is then written as

$$\varepsilon(\omega) = \varepsilon_\infty + \Delta\varepsilon (1 + i\omega\tau)^{-\beta} + \frac{Cm(\omega)}{\omega\varepsilon_0}, \tag{6}$$

where C is proportional to charge and the number of carriers participating in the conduction process. ε is taken in units of the permittivity ε_0 of free space.

§ 3. RESULTS

Horse myoglobin, as purchased from Sigma, was hydrated using a saturated KNO_3 solution, compressed into discs and sealed by a Teflon ring before measuring. The dielectric measurements were performed over a frequency range from 1 MHz to 1 GHz using a Hewlett–Packard impedance analyser. The temperature was controlled by a stream of cold nitrogen gas. Two samples were analysed: sample I ($h \approx 0{\cdot}36\,\mathrm{g\,g^{-1}}$) was inserted into the waveguide, immediately cooled to 217 K and then measured up to 272 K in steps of 6–7 K. Sample II ($h \approx 0{\cdot}32\,\mathrm{g\,g^{-1}}$) was measured from 299 up to 330 K in steps of 3–4 K.

Figure 2 shows ε' and ε'' of sample I for five different temperatures together with the fitted curves (eqn. (6)). Figure 3 displays the conductivity data for sample II. For the proton conduction process it was assumed that the elementary transfer step W_0 is controlled by the mean water dipole reorientation rate $W_0 = 1/\langle\tau\rangle = 1/\beta\tau$ (eqn. (6)), thus reducing the number of free parameters. The figures show that at both low temperatures (fig. 2 (*b*)) and low hydrations (curves 299 K (*a*) and 299 K (*b*) in fig. 3) the contribution of conduction to the signal, as depicted by the broken lines, diminishes within our frequency window. Correspondingly, under these conditions the broad distribution of water relaxation rates becomes evident; the fits yield $\beta = 0{\cdot}2$. At higher temperatures the cross-over from constant to dispersive conductivity at $\omega = \delta^2 W_0$ moves into the window. As W_0 is determined by $\langle\tau\rangle^{-1}$, this cross-over allows an estimate of δ. Figure 4 (*a*) shows the results for both samples, indicating an increase in

Fig. 2

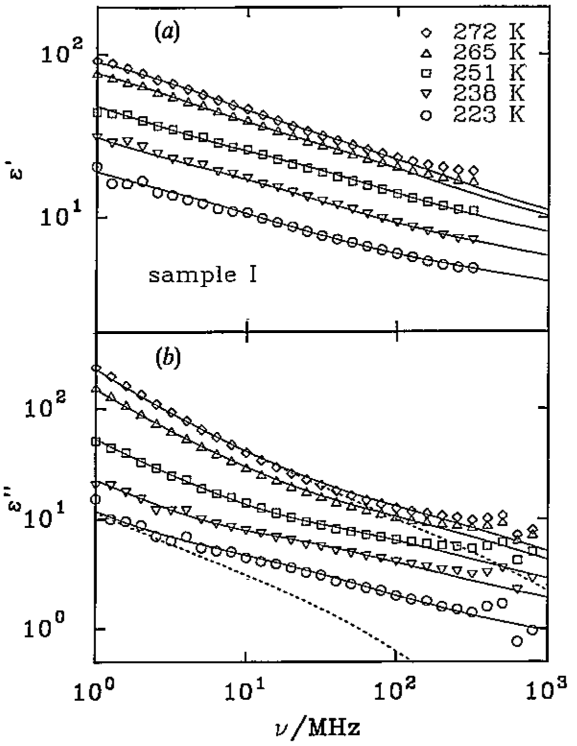

(*a*) Real and (*b*) imaginary part of $\varepsilon(\omega)$ for sample I with fitted curves from eqn. (6) for various temperatures.

Fig. 3

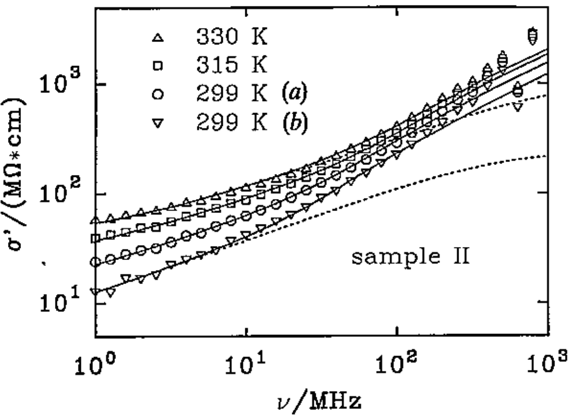

Conductivity $\sigma'(\omega)$ of sample II and fits according to eqn. (6). The two curves at 299 K refer to the measurements before (*a*) and after (*b*) heating the sample.

Fig. 4

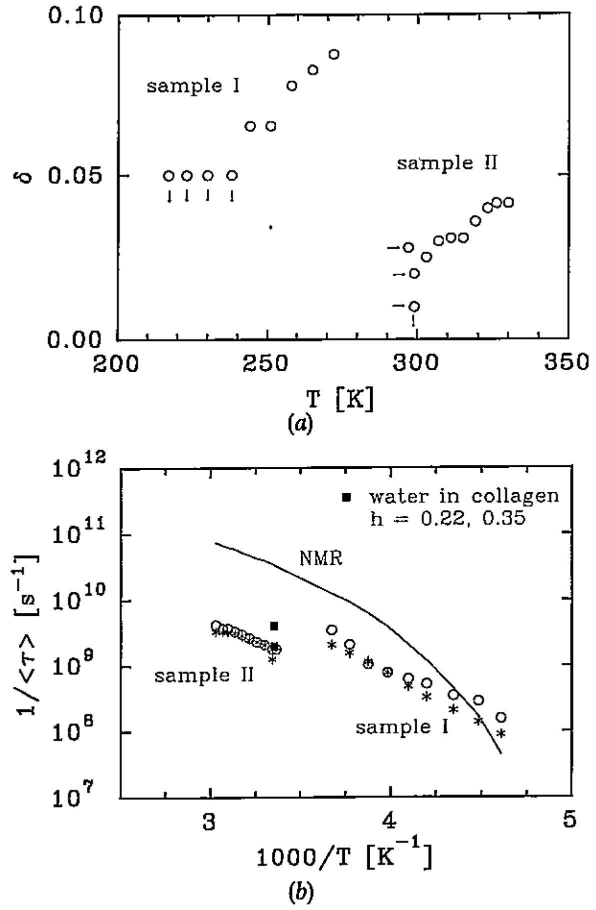

(*a*) Variation in the parameter δ with temperature for both samples. For the marked points the time of the measurement increases from top to bottom. The values marked with vertical arrows present upper limits. (*b*) Arrhenius plot of the fitted rates $W_0 = \langle\tau\rangle^{-1}$ in comparison with nuclear magnetic resonance data (F. Fujara and W. Doster, unpublished results) and dielectric measurements on hydration water in collagen (Shinyashiki *et al.* 1990).

the connectivity of the system with increasing temperature. The dependence on hydration is presented by the three points marked by horizontal arrows, the time of the measurement increasing from top to bottom. Symbols marked by vertical arrows represent upper limits for δ. The same general behaviour can be observed for the rates $W_0 = \langle\tau\rangle^{-1}$ shown in fig. 4(*b*) in comparison with data obtained from nuclear magnetic resonance measurements on samples of 0·45 g g^{-1} hydration. The different symbols correspond to two different sets of fitting parameters. The rates of sample I extrapolate to higher values at room temperature than those for sample II. This is in accord with the results of Shimyashiki *et al.* (1990), who found two adjoining water components, consistent with a description by one broad relaxation region and a slowing down of the mean relaxation rate with decreasing hydration.

§4. CONCLUSIONS

We have shown that the dielectric response of hydrated myoglobin can be explained by fast reorientation of water dipoles and a frequency-dependent conductance of protons along threads of hydrogen-bonded water molecules. It is encouraging, but not necessarily conclusive, that the conductivity term is reproduced by a simple percolation model. This result supports earlier studies focusing on the behaviour of the static conductivity (Careri *et al.* 1988). The range $\delta<0$ depicted in fig. 1 requires some comments. In the model the peak position shifts to higher frequencies, approximately $\delta^2 W_0$, for increasing negative δ because the average patch size decreases. This behaviour is in contradiction with low-hydration studies. However, in view of the observed cross-over from 3D (which we discuss) to 2D percolation (Careri *et al.* 1986), $\delta(3\mathrm{D})<0$ has to be replaced by $\delta'(2\mathrm{D})>0$ at low hydration. Further theoretical and experimental investigations are required to elucidate the relation of the elementary hopping step to water dipole reorientation. In particular, W_0 should be replaced by a distribution of rates reflecting the spread in the water relaxation times. Finally, we mention that the ^{2}H spin–lattice relaxation time of D_2O hydrated proteins also exhibits a square-root frequency dependence $T_1 \sim \omega^{0\cdot5}$ between 10^4 and 10^7 Hz (Schauer, Kimmich, and Nusser 1988). These workers suggest reorientation of the OD vector by translational diffusion of adsorbed water. If dielectric and nuclear magnetic resonance experiments reflect the same mechanism, one would conclude that the protons migrate in the form of H_3^+O ions.

REFERENCES

BÖTTCHER, C. J. F., and BORDEWIJK, P., 1978, *Theory of Electric Polarization* (Amsterdam: Elsevier).

BUNDE, A., and MAASS, P., 1991, *J. non-crystalline Solids*, **1022,** 131.

CARERI, G., and GIANSANTI, A., 1984, *Lett. Nuovo Cim.*, **40,** 193.

CARERI, G., GERACI, M., GIANSANTI, A., and RUPLEY, J. A., 1985, *Proc. Natl. Acad. Sci. U.S.A.*, **82,** 5342.

CARERI, G., GIANSANTI, A., and RUPLEY, J. A., 1986, *Proc. Natl. Acad. Sci. U.S.A.*, **83,** 6810; 1988, *Phys. Rev.* A, **37,** 2703.

DOSTER, W., and SCHIRMACHER, W., 1990, *Biophys. J.*, **57,** 681; 1991, *Comm. Theor. Biol.*, **2,** 261.

DOSTER, W., SCHIRMACHER, W., and SETTLES, M., 1990, *Biophys. J.*, **57,** 681.

HAWKES, J. J., and PETHIG, R., 1988, *Biochim. biophys. Acta*, **952,** 27.

MOVAGHAR, B., and SCHIRMACHER, W., 1981, *J. Phys.* C, **14,** 859.

SCHAUER, G., KIMMICH, R., and NUSSER, W., 1988, *Biophys. J.*, **57,** 397.

SHINYASHIKI, N., ASAKA, N., MASHIMO, S., YAGIHARA, S., and SASAKI, M., 1990, *Biopolymers*, **29,** 1185.